Appendix to:

Cellular senescence leads to progressive cell death via the INK4a-RB pathway in naked mole-rats

Yoshimi Kawamura, Kaori Oka, Takashi Semba, Mayuko Takamori, Yuki Sugiura, Riyo Yamasaki, Yusuke Suzuki, Takeshi Chujo, Mari Nagase, Yuki Oiwa, Shusuke Fujioka, Sayuri Homma, Yuki Yamamura, Shingo Miyawaki, Minoru Narita, Takaichi Fukuda, Yusuke Sakai, Takatsugu Ishimoto, Kazuhito Tomizawa, Makoto Suematsu, Takuya Yamamoto, Hidemasa Bono, Hideyuki Okano and Kyoko Miura

Table of contents

Appendix Figure S1

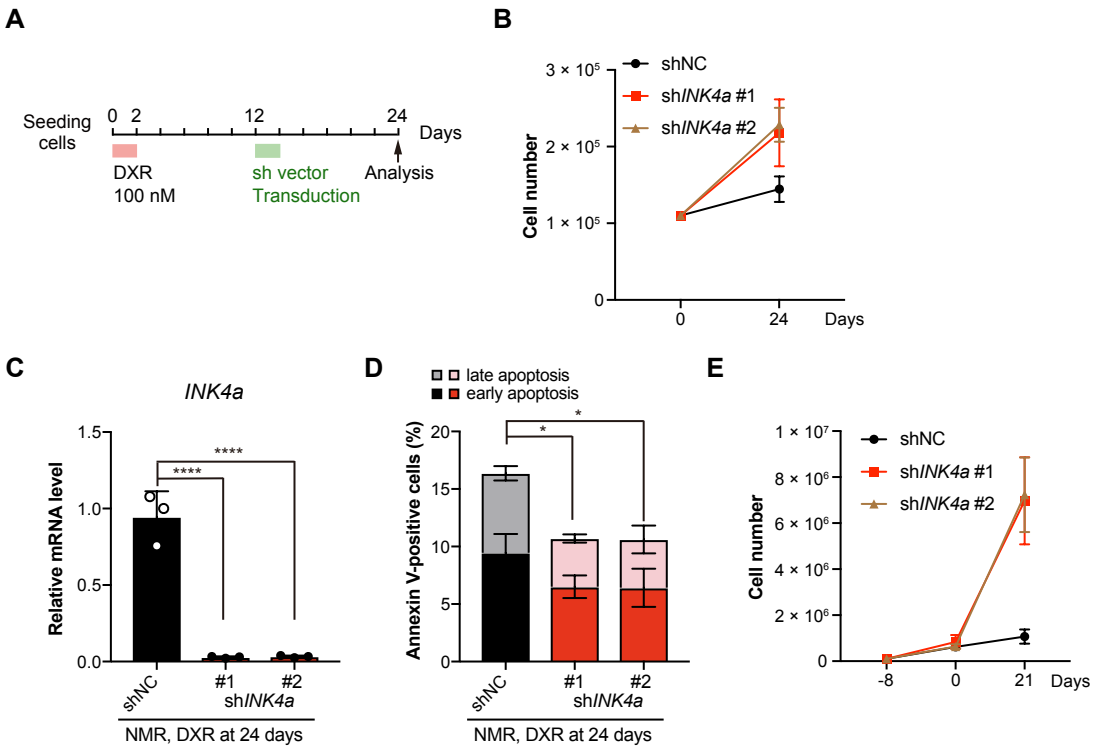

Appendix Figure S1. Induction of cellular senescence by DNA damage leads to delayed, progressive cell death in an *INK4a*-dependent manner in NMR fibroblasts.

(**A**) Scheme for doxorubicin (DXR) treatment before *INK4a* knockdown.

(**B**) Proliferation of NMR fibroblasts treated with DXR before *INK4a* knockdown.

(**C**, **D**) qRT-PCR analysis of the expression of *INK4a* normalized to *ACTB* mRNA levels (**C**) and quantification of Annexin V-positive cells (%) (Annexin V+/PI– as early apoptotic and Annexin V+/PI+ double-positive as late apoptotic) (**D**) in NMR fibroblasts treated with DXR before *INK4a* knockdown.

(**E**) Proliferation of NMR fibroblasts treated with DXR after *INK4a* knockdown (the same treatment as in Fig 1**I**). The DXR treatment was performed from day 0.

* $P < 0.05$, **** $P < 0.0001$; ns, not significant. One-way ANOVA followed by Dunnett's multiple comparison test for (**C** and **D**).

Data are expressed as the mean ± SD from $n = 3$ biological replicates.

Appendix Figure S2

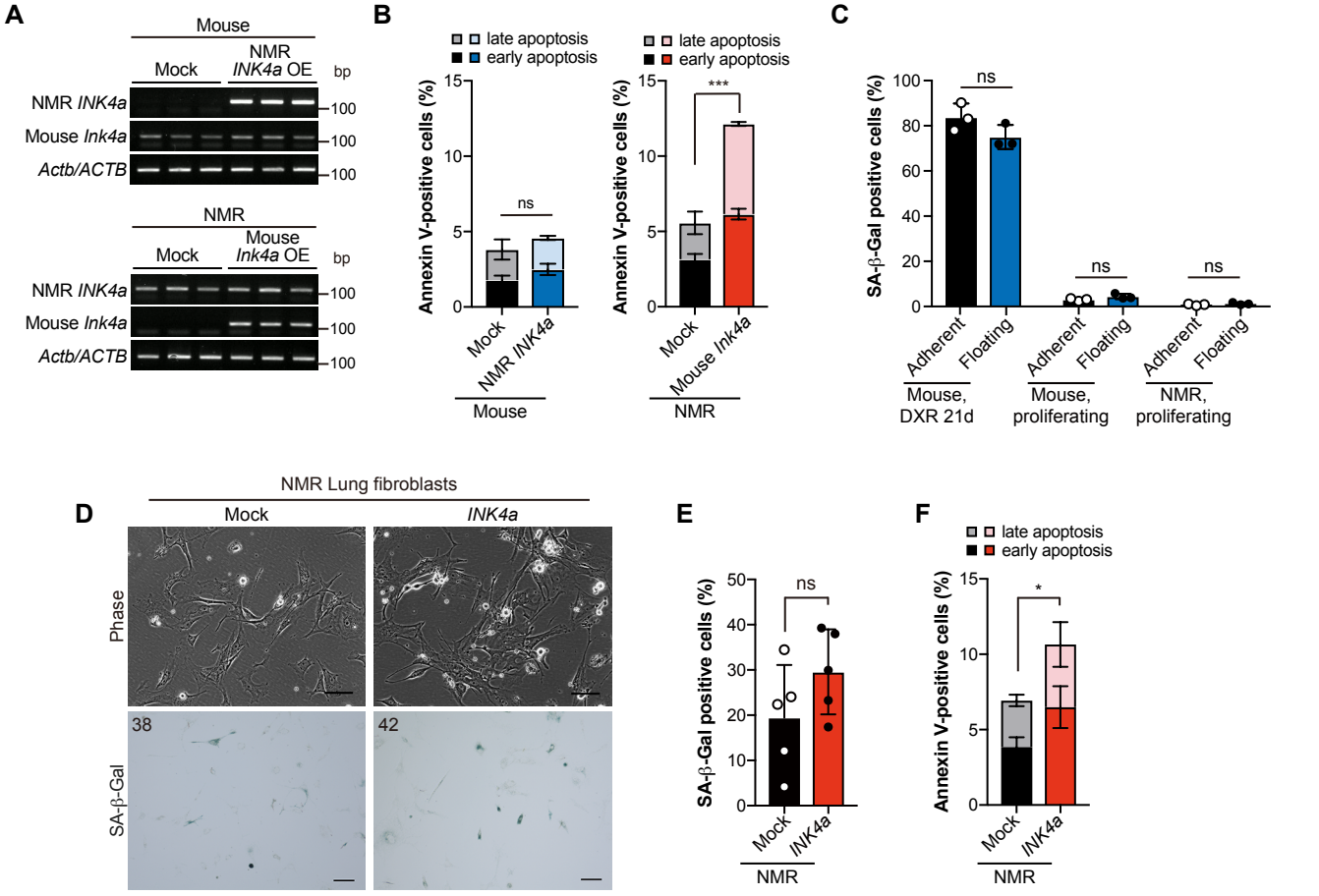

Appendix Figure S2. *INK4a* transduction results in progressive cell death in NMR skin and lung fibroblasts.

(**A**) RT-PCR analysis of expression of mouse *Ink4a* and NMR *INK4a* in NMR *INK4a*-transduced mouse fibroblasts or mouse *Ink4a*-transduced NMR fibroblasts at 12 days after transduction. OE; overexpression.

(**B**) Quantification of Annexin V/PI-positive cells (%) (Annexin V+/PI– as early apoptotic and Annexin V+/PI+ double-positive as late apoptotic) at 12 days after transduction of NMR *INK4a* into mouse fibroblasts or mouse *Ink4a* into NMR fibroblasts. Data are expressed as the mean ± SD from *n* = 3 biological replicates.

(**C**) Quantification of SA-β-Gal-positive cells in the adherent living cell population and floating dead cell population at 24 h after UV-C irradiation. Data are expressed as the mean ± SD from *n* = 3 biological replicates.

(**D**) Cell morphology and SA-β-Gal activity in NMR-lung fibroblasts at 12 days after *INK4a* transduction. Scale bar, 100 μm. The number in the upper left corner indicates Hoechst-positive nuclei.

(**E**–**F**) Quantification of SA-β-Gal-positive cells (%) (**E**), and quantification of Annexin V-positive cells (Annexin V+/PI– as early apoptotic and Annexin V+/PI+ double-positive as late apoptotic) (**F**) in NMR lung fibroblasts at 12 days after INK4a transduction (%). Data are expressed as the mean ± SD from *n* = 5 biological replicates.

* $P < 0.05$, *** $P < 0.001$; ns, not significant; unpaired *t*-test for (**B**, **C**, **E**, and **F**).

Appendix Figure S3

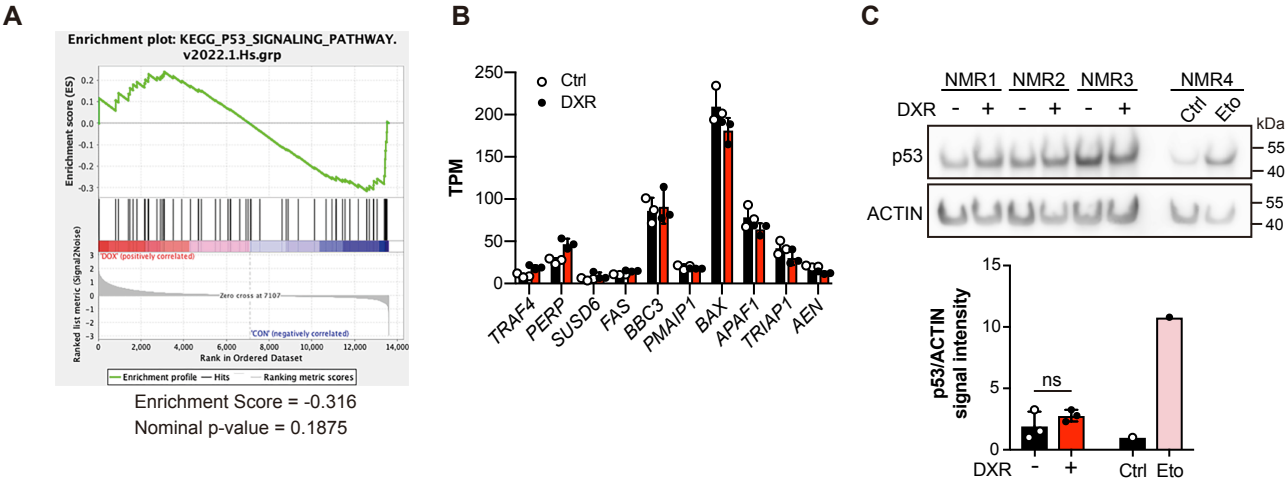

Appendix Figure S3. Doxorubicin treatment results in progressive cell death independent of p53 in NMR fibroblasts.

(**A**) Gene set enrichment analysis (GSEA) plot depicting p53 signaling pathway genes in control (Ctrl) versus NMR fibroblasts 21 days after doxorubicin (DXR) treatment.

(**B**) Expression levels of p53 target genes (transcripts per million, TPM) in Ctrl and NMR fibroblasts 21 days after DXR treatment.

(**C**) Western blot analysis and quantitative data of p53 in NMR fibroblasts 21 days after DXR treatment or 4 days after 200 μM of etoposide (Eto) treatment. ACTIN was used as a loading control. Data are expressed as the mean ± SD from *n* = 3 biological replicates. ns, not significant.

Unpaired *t*-test versus DXR- for **C**.

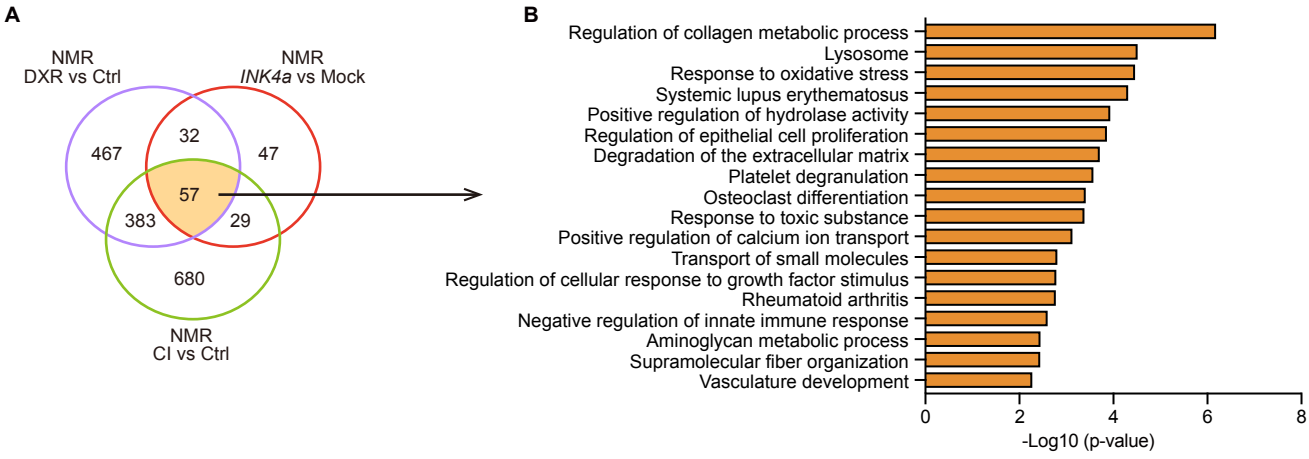

Appendix Figure S4. Commonly upregulated genes in DXR-treated, *INK4a*-transduced, and CI-induced NMR fibroblasts.

(**A**) Venn diagram showing the differentially expressed genes (DEGs, >1.5-fold in DXR-treated, *INK4a*-transduced, or CI-induced NMR fibroblasts) identified from comparisons of Ctrl and DXR-treated NMR fibroblasts at 21 days after treatment, mock and *INK4a*-transduced NMR fibroblasts at 12 days after transduction, or Ctrl and CI-induced NMR fibroblasts at 28 days after induction. Data were obtained from $n = 3$ biological replicates.

(**B**) Top 18 enriched gene ontology (GO) terms and KEGG pathways obtained using Metascape analysis of the 57 common genes in **A**.

Appendix Figure S5

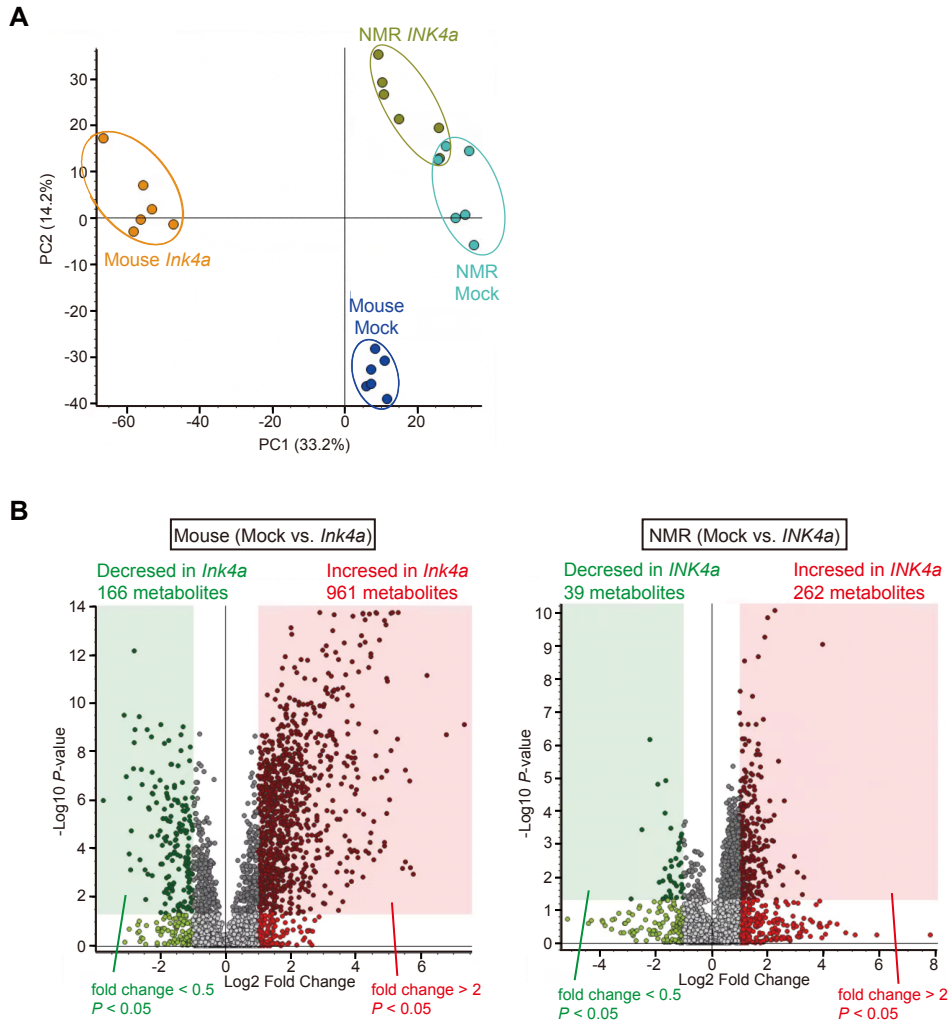

Appendix Figure S5. Metabolome analysis in *INK4a*-transduced mouse or NMR fibroblasts.

(**A**) PCA plot of metabolome differences in mouse or NMR fibroblasts at 12 days after *Ink4a/INK4a* or mock vector transduction. Data were obtained from two technical replicates for each primary fibroblast culture (n = 3 biological replicates).

(**B**) Volcano plots of metabolome differences in mouse or NMR fibroblasts at 12 days after *Ink4a/INK4a* transduction compared with mock. The x-axis shows the fold change in metabolite levels between different samples, and the y-axis shows the statistical significance of the differences. Significantly increased and decreased metabolites are highlighted in red and green, respectively.

Appendix Figure S6

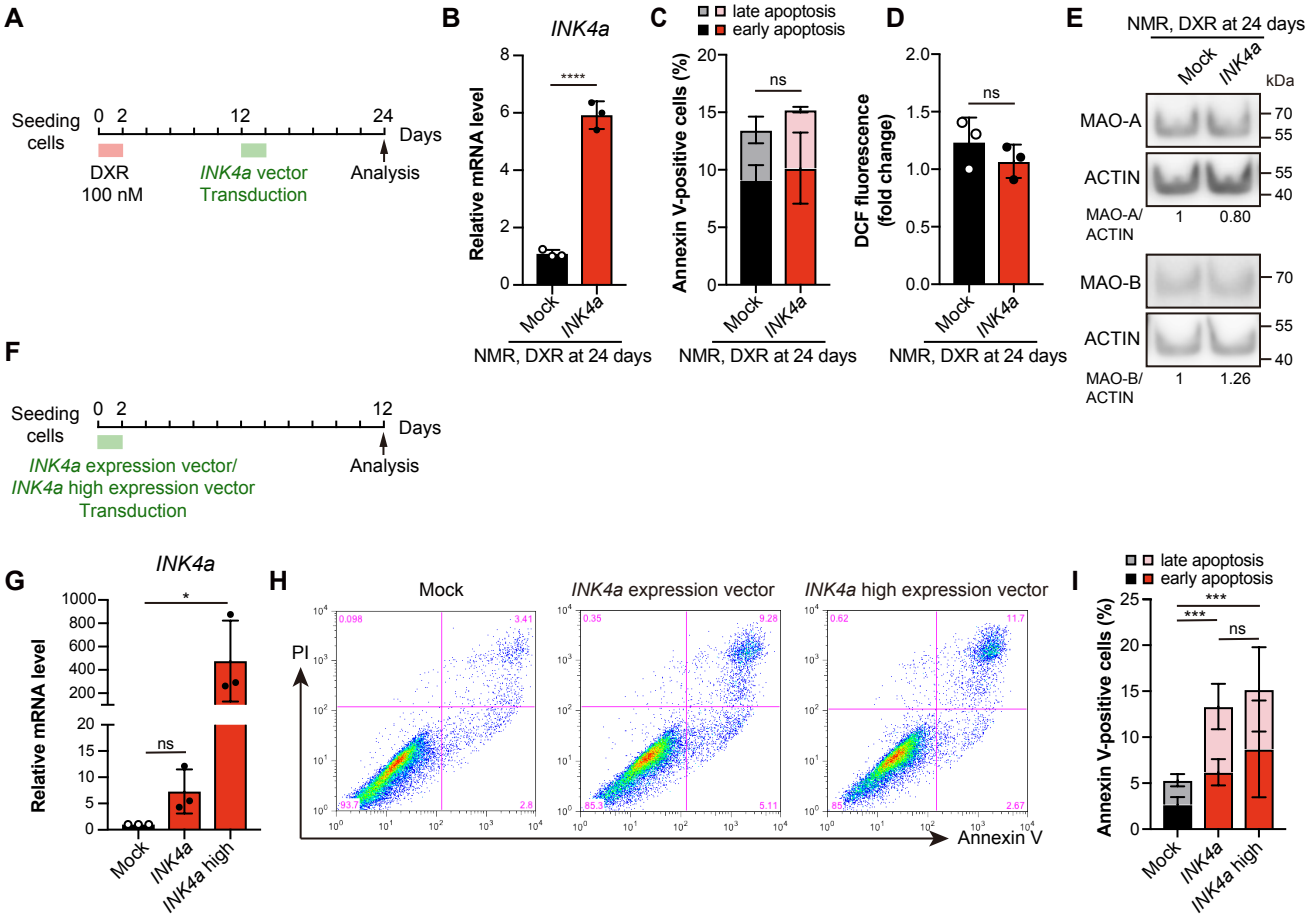

Appendix Figure S6. Further increasing *INK4a* expression does not further enhance cell death in senescent NMR-fibroblasts.

(**A**) Scheme for *INK4a* overexpression after doxorubicin (DXR) treatment in NMR fibroblasts.

(**B**–**D**) qRT-PCR analysis of the expression of *INK4a* normalized to *ACTB* mRNA levels (**B**), quantification of Annexin V-positive cells (%) (Annexin V+/PI– as early apoptotic and Annexin V+/PI+ double-positive as late apoptotic) (**C**), and quantification of reactive oxygen species (ROS) using 2',7'-dihydrodichlorofluorescin diacetate (DCFH-DA) (**D**) in DXR-treated NMR fibroblasts transduced with *INK4a*.

(**E**) Western blot analysis of monoamine oxidase (MAO)-A and MAO-B in NMR fibroblasts at 24 days after DXR treatment. ACTIN was used as a loading control. Numbers below the gel images indicate quantification of MAO-A or -B/ACTIN intensity (n = 3 average).

(**F**) Scheme for *INK4a* overexpression in NMR fibroblasts using vectors with different expression levels.

(**G**) qRT-PCR analysis of the expression of *INK4a* normalized to *ACTB* mRNA levels at 12 days after *INK4a* transduction.

(**H**) Representative FACS profiles of Annexin V/PI staining of NMR fibroblasts 12 days after mock or *INK4a* transduction.

(**I**) Quantification of Annexin V-positive cells (%) (Annexin V+/PI– as early apoptotic and Annexin V+/PI+ double-positive as late apoptotic) at 12 days after *INK4a* transduction.

* $P < 0.05$; *** $P < 0.001$; **** $P < 0.0001$; ns, not significant. Unpaired t-test versus control for (**B**, **C** and **D**). One-way ANOVA followed by Dunnett's multiple comparison test for (**G**). One-way ANOVA followed by Sidak's multiple comparisons test for (**I**). Data are expressed as the mean ± SD from n = 3 biological replicates.

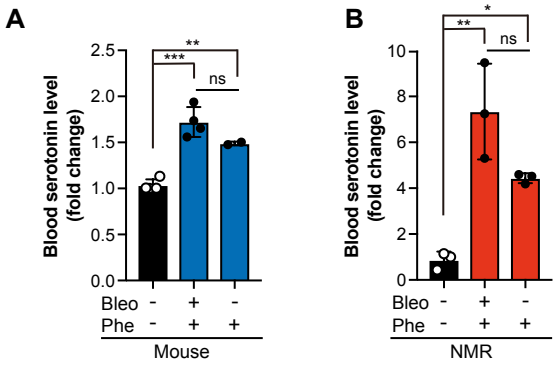

Appendix Figure S7. Phenelzine administration increases blood serotonin levels.

(**A**) Blood serotonin levels in mice treated with bleomycin (Bleo) and phenelzine (Phe) or Phe alone. Data are expressed as the mean ± SD from $n = 4$ biological replicates except for Phe only ($n = 2$).

(**B**) Blood serotonin levels in NMRs treated with Bleo and Phe or Phe alone. Data are expressed as the mean ± SD from $n = 3$ biological replicates.

* $P < 0.05$, ** $P < 0.01$, *** $P < 0.001$. One-way ANOVA followed by Tukey's multiple comparison test.

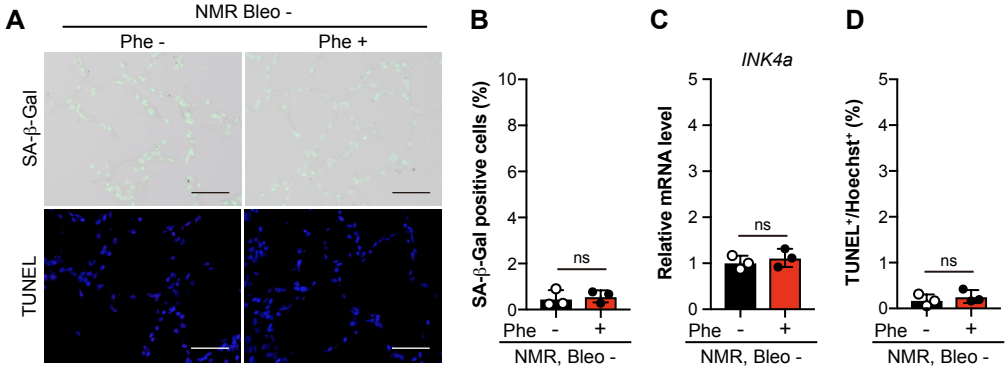

Appendix Figure S8. Phenelzine administration alone does not affect cell death or cellular senescence in NMR lungs.

(**A**) SA-β-Gal activity (SA-β-Gal, blue; nuclei, green) and TUNEL staining (TUNEL, red; nuclei, blue) in the lungs of NMRs treated with Phe for 5 consecutive days.

(**B**–**D**) Quantification of SA-β-Gal-positive cells (%) (**B**), qRT-PCR analysis of *INK4a* expression normalized to *ACTB* mRNA levels (**C**), quantification of TUNEL-positive cells (%) (**D**) in NMR lungs treated with Phe for 5 consecutive days.

Scale bar, 50 μm. ns, not significant. Unpaired *t*-test versus Phe- for (**B**–**D**). Data are expressed as the mean ± SD from *n* = 3 biological replicates.

Appendix Table S1. Naked mole-rats used in this study.

Experiments	ID	Sex	Birth	Day of sacrifice or sample collection	Use
in vitro experiments	2B28	M	2018.7.31	2019.7.17	Skin fibroblasts culture
	2E20	F	2017.06.16	2018.10.2	Skin fibroblasts culture
	2E4	F	2016.12.5	2020. 6. 13	Skin fibroblasts culture
	2EX	M	2016-2017	2018.6.16	Skin fibroblasts culture
	C42	M	2017.1.5	2018.8.16	Skin fibroblasts culture, RNA sequencing
	CG3	M	2018.12.14	2020.1.29	Skin fibroblasts culture
	CG7	M	2018.12.14	2020.1.29	Skin fibroblasts culture
	D2	ND	2009-2010	2011.9.21	Skin and lung fibroblasts culture, RNA sequencing
	D23	M	2016.8.16	2017.9.26	Skin fibroblasts culture
	D43	M	2019.12.3	2020.12.9	Skin fibroblasts culture, RNA sequencing
	G24	F	2014.9.5	202015.9.3	Skin fibroblasts culture
	GH30	F	2019.12.11	2020.10.29	Skin fibroblasts culture, RNA sequencing
	GH32	F	2019.12.11	2020.10.30	Skin fibroblasts culture
	GH33	F	2019.12.11	2020.10.28	Skin fibroblasts culture, RNA sequencing
	H17	ND	2010-2011	2012.12.16	Skin and lung fibroblasts culture
	H44	F	2015.8.25	2016.12.15	Skin fibroblasts culture, RNA sequencing
	H45	M	2015.8.25	2016.12.15	Skin fibroblasts culture, RNA sequencing
	L14	F	2014.9.8	2015.12.10	Skin fibroblasts culture, RNA sequencing
	L4	M	2013.12.10	2015.3.10	Skin fibroblasts culture
	M15	F	2013.5.13	2016.8.1	Lung fibroblasts culture
	O13	F	2012.10.11	2016.10.28	Lung fibroblasts culture
	R14	M	2016.8.8	2017.7.19	Lung fibroblasts culture
	Y26	M	2017.3.24	2018.8.16	Skin fibroblasts culture
Biopsy	R18	F	2016.8.8	2017.9.12	RNA extraction
	DR9	M	2021.10.15	2023.2.9	RNA extraction
	DR13	M	2021.10.15	2023.2.9	RNA extraction
	D78	M	2021.7.1	2023.2.10	RNA extraction
	F1	F	2002.6.6	2017.8.26	RNA extraction
	H4	M	2008.1.17	2023.2.9	RNA extraction
	H3	M	2008.1.17	2023.2.10	RNA extraction
	G2	M	2008.1.17	2023.2.11	RNA extraction
Bleomycin administration	LR1	M	2021.6.19	2022.8.26	Histology and RNA extraction
	LR2	M	2021.6.19	2022.8.26	Histology and RNA extraction
	LR3	M	2021.6.19	2022.8.26	Histology and RNA extraction
	D47b	M	2021.4.8	2022.8.31	Histology and RNA extraction
	D51b	M	2021.4.8	2022.8.31	Histology and RNA extraction
	Y56b	M	2020.6.19	2022.8.4	Histology and RNA extraction
	CY10	M	2020.7.8	2022.9.7	Histology and RNA extraction
	CY15	M	2020.10.24	2022.9.7	Histology and RNA extraction
	CY23	M	2020.10.24	2022.9.7	Histology and RNA extraction
	D48b	M	2021.4.8	2022.9.14	Histology and RNA extraction
	D49b	M	2021.4.8	2022.9.14	Histology and RNA extraction
	D50b	M	2021.4.8	2022.9.14	Histology and RNA extraction
Bleomycin and phenelzine administration	BC40	M	2021.11.3	2023.1.11	Histology and RNA extraction
	BC43	M	2021.11.3	2023.1.11	Histology and RNA extraction
	BC44	M	2021.11.3	2023.1.11	Histology and RNA extraction
Phenelzine administration	BC39	M	2021.11.3	2023.2.14	Histology and RNA extraction
	BC46	M	2021.11.3	2023.2.14	Histology and RNA extraction
	D40b	F	2019.10.4	2023.2.19	Histology and RNA extraction
Sham control	DR2	M	2021.6.23	2022.8.31	Histology and RNA extraction
	DCG2	M	2021.5.2	2022.8.31	Histology and RNA extraction
	Y57b	M	2020.6.19	2022.8.4	Histology and RNA extraction

Appendix Table S2. Primers used in this study.

Gene	Primer	Sequcence (5'-3')
Ink4a (Mouse)	Forward	GTGTGCATGACGTGCGGG
	Reverse	GCAGTTCGAATCTGCACCGTAG
p21 (Mouse)	Forward	TCCCGTGGACAGTGAGCAGTTG
	Reverse	CGTCTCCGTGACGAAGTCAAAG
INK4a (NMR)	Forward	CGCCCAATGCCCGGAACCGTTT
	Reverse	GCGCCGCGTCATGCACCGGTA
INK4a (NMR)	Forward	GACCCGAACTGCGCTGACCCT
	Reverse	CCGCGTCATGCACCGGTAGTGTGA
p21 (NMR)	Forward	ACCTGTCGCTGTCCTGCACCCTTG
	Reverse	CGTCATGCTGGTCTGCCGCCGTT
ACTB	Forward	AGACCTTCAACACCCCAGCCATGT
	Reverse	GGCCAGCCAGGTCCAGACGCAG
SV40LT	Forward	GCTGACTCTCAACATTCTACTCCTC
	Reverse	TAGCAGACACTCTATGCCTGTGTGG